Modeling the Creep Behavior of Torsional Springs

A. Ramesh, K. Bose and K.M. Lawton

Department of Mechanical Engineering and Engineering Science

The University of North Carolina at Charlotte

Abstract: *A finite element model is developed to investigate the instantaneous as well as long-term (time-dependant) structural response of a pre-loaded torsional spring. Torsional springs belong to a class of spiral springs that are commonly made out of Elgiloy - an alloy of Cobalt, Chromium, Nickel and Iron. Elgiloy has very high yield strength, and is commonly used as a spring material in clocks. The research involves development of a detailed component-level model, using Abaqus/Standard, to investigate the instantaneous static moment-rotation response, and the long-term stress relaxation response of the spring system, along with, understanding the sensitivity of this response on the various design parameters. Frictional self contact, large deformation and nonlinear material behavior (plasticity and creep) are among the major challenges in solving this problem. The modeling effort also involves understanding the experimentally-observed hysteresis associated with the cyclic moment versus rotation response, and development of simple analytical models which can approximately describe the structural response of a typical torsional spring system with varying parameters.*

Keywords: *Aging, Creep, Freshly-Formed, Frictional Self-Contact, Hysteresis, Large-Deformations, Plasticity, and Torsional Spring.*

1. Introduction

Previous research conducted on elgiloy-based springs focused on measuring the properties of the elgiloy material (including creep) from a material science perspective (Assefpour-Dezfuly, 1984, 1985) and/or studies conducted on the load relaxation response of elgiloy based helical coil springs (Dykhuizen, 2004). There is little or no reference in the literature on the mechanical behavior and/or design of torsional springs.

Torsional springs are typically used to provide a certain value of torque for a specified rotation. The research presented here is part of a broader program that also has an experimental component (Lawton, 2007). However, experiments have their limitations in measuring the stress relaxation response over extended service lives--of the order of several years or decades. Furthermore, a large number of experiments would be needed to gain sufficient insight into certain aspects of the complex spring response, such as the dependence of performance on the coefficients of friction between the various contacting parts of the spring. Numerical modeling can provide some of the critical insights in this regard.

The primary objective of this research is to develop a detailed finite element model that will accurately describe the characteristics of a torsional spring system, and predict its response through numerical modeling. It is assumed that the response of the spring is a strong function of the base state of the spring (state of residual stresses, for example). The base state is the state of the spring at the end of the “spring forming” process. With the above in mind, the model tracks the process of forming the spring, and captures the time-independent static (moment-rotation) as well as the time-dependent relaxation responses about a pre-loaded state. The forming process and the additional wind-ups are modeled as non-linear static processes, while the long-term relaxation is modeled as a transient static (visco) process.

2. Theory

Previous research conducted on time-dependant response has been confined to 'material creep', which is broadly defined as the response of a stressed material as a function of time. Temperature appears to play a significant role in this process. However, in some materials (e.g., Elgiloy) significant creep can even occur at room temperatures. As a result, springs made of such materials may relax their instantaneous loads over a period of time. Such a phenomenon may be termed as 'structural creep', which is defined as the influence of material creep on the complex response of a structure. Here, the structure under consideration is a loaded torsional spring with the load relaxing over a period of time. This process can lead to significant torque relaxation depending on the complexity of the spring and the time period over which it is allowed to relax. The creep involved here is treated as secondary creep because of the time scales involved. Figure 1 shows a schematic of the strain-time curve for a typical material creep test.

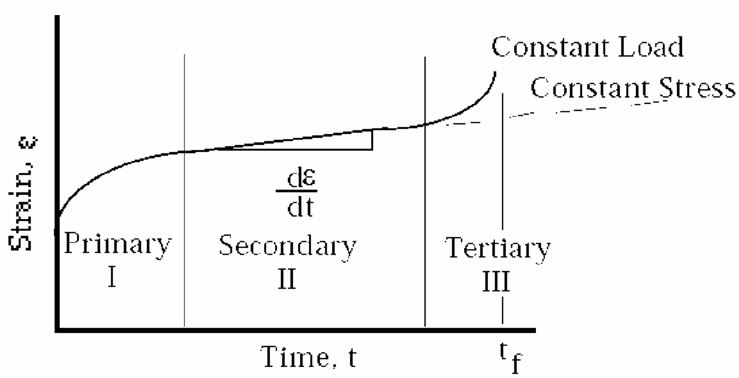

Figure 1. A schematic of a strain-time curve for a material creep test.

3. Design Specifications

The clock spring assembly, as shown in Figure 2, comprises of a flat elgiloy strip (wire), an arbor of radius 1 mm onto which the flat wire is wrapped upon, and a rigid cup with an inner radius of approximately 2.7 mm which houses the entire assembly. The flat elgiloy wire is 0.1 mm thick, 1 mm wide and 116 mm long, and has 85% cold-work reduction with the associated yield strength of approximately 240 ksi (Dalder, 2003) (≈1655 MPa). Approximately 3.5 mm of the strip is annealed and attached onto the centered arbor (concentric with the cup). The springs are required to generate torques of approximately 2.9 ± 0.5 N.mm at 1 revolution and 4.35 ± 0.55 N.mm at 2.25 revolutions.

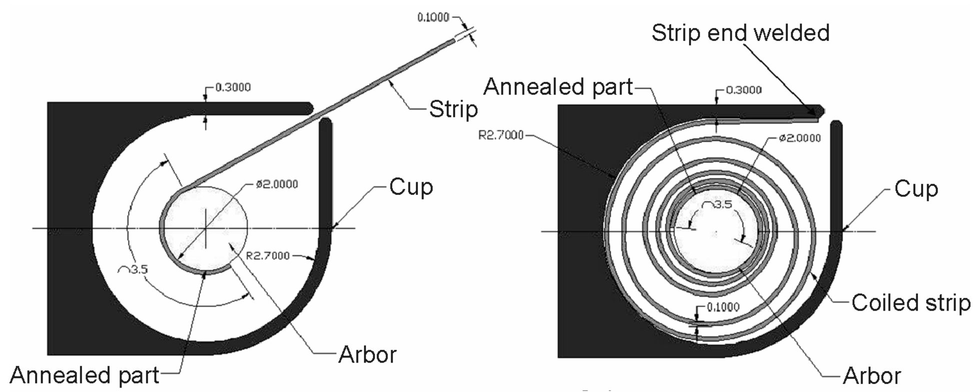

Figure 2. Schematic of the clock spring assembly before and after forming.

4. Procedures and Results

Abaqus/Standard is used for modeling this problem. Complexities in solving this problem include material non-linearity involving plasticity and creep, geometric non-linearity associated with large deformations, and boundary non-linearity involving frictional self contact. Non-default solution control algorithms were necessary to address some of these complexities. In addition, viscous stabilization is used to remove local instabilities (associated with a long slender structure that is relatively unconstrained) during the forming process, and softened normal contact to reduce the large discontinuities in contact pressures arising in self contact. The model uses the 2-D solid continuum element- CPE4R, i.e., a bi-linear quadrilateral element used in plain strain problems with reduced integration (Abaqus/Standard Analysis User's Manual, v 6.7). The influence of material hardening and the effect of lubrication are also investigated. The problem requires four major levels of modeling effort; namely, the initial forming process, additional wind-ups of the spring to determine the instantaneous static moment-rotation response, cyclic loading and unloading to determine the hysteresis response, and the long-term relaxation response. The methodology used at each level and the results obtained are described in the following sections.

4.1 Forming process

The specific objectives for modeling the spring forming process are, capturing the (i) residual stresses, (ii) plastic strains and (iii) contact conditions, which describe the “state” of the spring at the end of the forming process. The forming process can be further divided into two steps; namely, (i) the winding phase, and (ii) the arbor release phase.

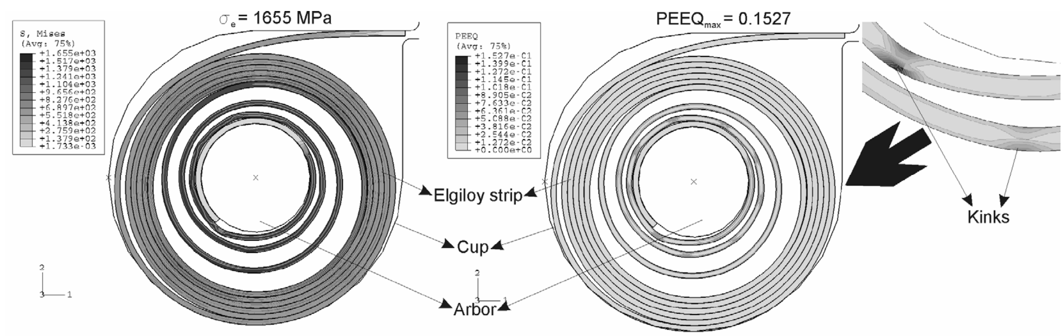

Figure 3. Contour plots for von-Mises stress and equivalent plastic strain at the end of the winding phase of the forming process.

During the winding phase, the arbor (initially concentric with the cup) is rotated so as to pull the flat wire into a spiral form inside of the cup. At the end of this phase, about 2 mm of the rear end of the strip is welded onto the cup opening or 'nose'. Any translational motion of the arbor is prevented during this phase. Figure 3 shows contour plots for von-Mises stress and equivalent plastic strain at the end of the initial winding. The spring coils were found to undergo large plastic deformation during this process, leading to the formation of 'kinks' or hot-spots (as shown in the inset of Figure 3).

During the arbor-release phase, all degrees of freedom in the arbor (at the end of winding) are released. Figure 4 shows a comparison of the actual clock spring profile after it is formed (wound and released), with the corresponding finite element model. It can be seen that the FE model is able to accurately capture the actual released profile of the spring, both in terms of the position of the arbor at the end of its release, and the alignment of the majority of the coils to the outer cup.

A detailed study was conducted on the spring system to understand the physics of the problem. The results attributed the occurrence of periodic 'kinks' or hot spots in the formed spring to the periodic “oscillatory” motion of the strip as it is pulled into the cup, during the initial winding phase. The already formed kinks further lead to the formation of more kinks due to self contact. Friction was found to increase the strain level in these hot spots.

With the goal of obtaining the most accurate physical solution, optimization of the spring model was performed by reducing the viscous stabilization factor. It was observed that the finite element model best matched the actual clock spring profile for the lowest factor of stabilization used.

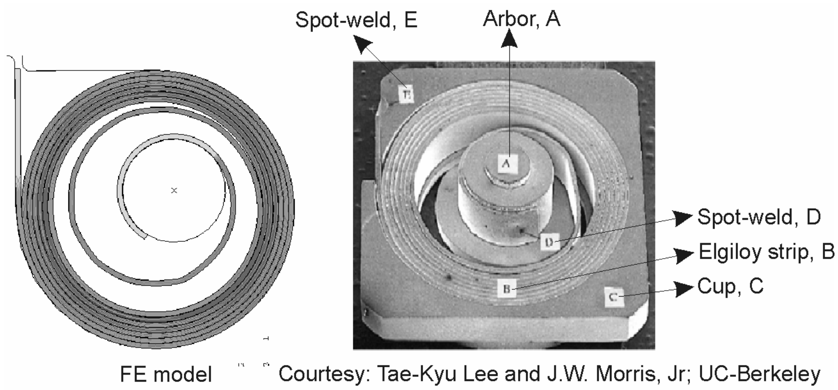

Figure 4. Comparison of the real formed profile of the spring (right) with the finite element model, at the end of arbor-release.

The results provided in the following sections correspond to the lowest factor of stabilization.

4.2 Instantaneous moment-rotation response at additional wind-ups

The primary objective of this modeling phase is to predict the instantaneous static moment versus rotation response of the spring system. This is accomplished by superposing additional rotations on the formed spring, and computing the corresponding reaction moments. Wind-up levels of 1 revolution and 2.25 revolutions were of primary interest in this project. The torque readings that were obtained at these levels of wind-up were found to be in good agreement with the experimental results. Table 1 shows a comparison of the torque readings for various levels of loading, and for different cases of material plasticity and friction. The design specifications are also provided.

Based on the results obtained, material hardening was found to increase the torque readings significantly, whereas lubrication was found to reduce them, although to a lower extent. This behavior suggests that the residual stresses (resulting from the forming process) and frictional self-contact (stick-slip behaviors) have a significant influence on the structural response of the spring system.

Note that the term 'Perfect lubrication', referred to in Table 1, corresponds to a coefficient of friction for self contact of $\mu = 0$*, whereas 'No lubrication' corresponds to* $\mu = 0.13$.

Levels of wind-up	Torque readings obtained from the FE model (N.mm)				Design Specifications (N.mm)
	Perfect Plasticity		Hardening Plasticity		
	Perfect lubrication	No lubrication	Perfect lubrication	No lubrication	
End of winding	3.835	3.861	4.149	4.296	-Not applicable-
Arbor release	0.000	0.000	0.000	0.000	-Not applicable-
1 revolution	3.521	3.787	4.142	4.377	2.9 $\pm$ 0.5
2.25 revolutions	4.398	4.561	4.785	5.142	4.35 $\pm$ 0.55

Table 1. Comparison of torque readings from the FE model with design specifications.

The moment-rotation plots for the additional wind-ups show evidence of a strong non-smooth response, as shown in Figures 5 - a & b. This phenomenon was found to be attributed to the "pinning" effect of the kinks on the neighboring coils during self contact, although it is still under investigation. It was also observed that, for the case of 1 revolution, the spring coils were pre-dominantly elastically loaded, whereas for 2.25 revolutions, the majority of the coils were plastically loaded (as evident from the maximum values of von-Mises stress for the two wind-ups, as shown in Figures 5 - a & b).

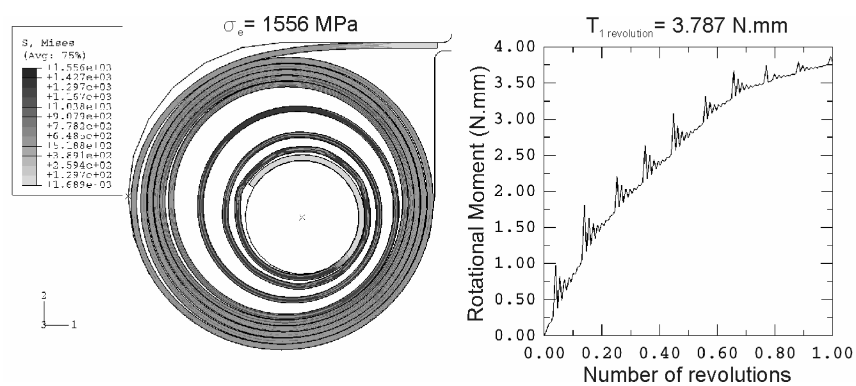

a. 1 revolution case.

Figure 5. Moment-rotation plots for additional wind-ups.

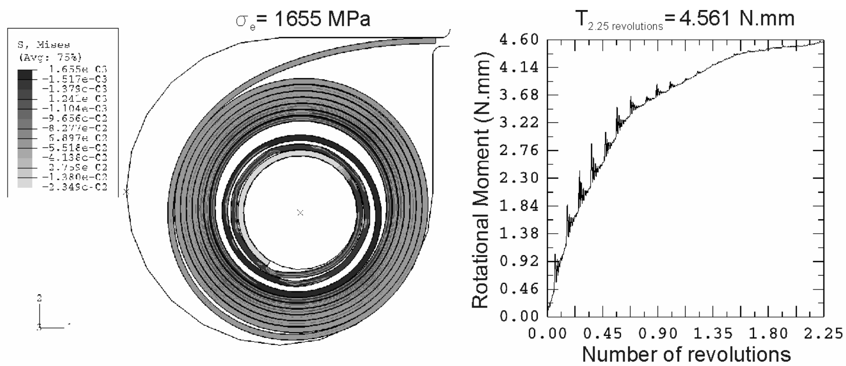

b. 2.25 revolutions case.

Figure 5. Moment-rotation plots for additional wind-ups.

The influence of viscous stabilization on the moment-rotation response was also investigated. Values for the factor of stabilization in the range of $5E-05 \leq F \leq 3E-04$ were found to generate converging solutions. The corresponding torque readings increased initially with reducing factor of stabilization- F , and then stabilized to a point beyond which the simulations failed to converge. Figure 6 shows variation of the instantaneous moment with the factor of stabilization, for additional wind-ups of 1 and 2.25 revolutions, respectively.

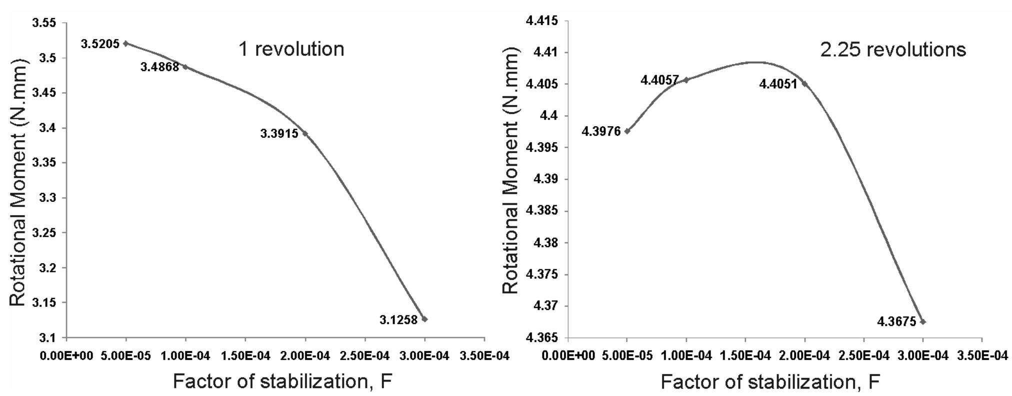

Figure 6. Comparison of torque readings for varying factors of stabilization.

The lowest factor of stabilization for which the simulations converged was for $F = 5E-05$.

4.3 Cyclic moment versus rotation (hysteresis) response

The objective of this modeling effort is to better understand the experimentally observed hysteresis associated with cyclic moment versus rotation response. This is accomplished by subjecting the formed spring to rotation controlled loading and unloading cycles. The torque readings so obtained indicated a remarkable amount of hysteresis. Apart from the torque lost (at a fixed value of rotation) due to hysteresis between a wind and unwind (within a cycle), torque lost between successive winds was also measured. For either case, the lost torque was calculated as an average of the difference in the corresponding torque readings at various rotational positions of the arbor.

The influence of material hardening on the cyclic-moment-rotation response was also investigated. Figure 7 shows cyclic loading-unloading plots obtained from the FE model for either cases of material plasticity (at 2.25 revolutions of the arbor).

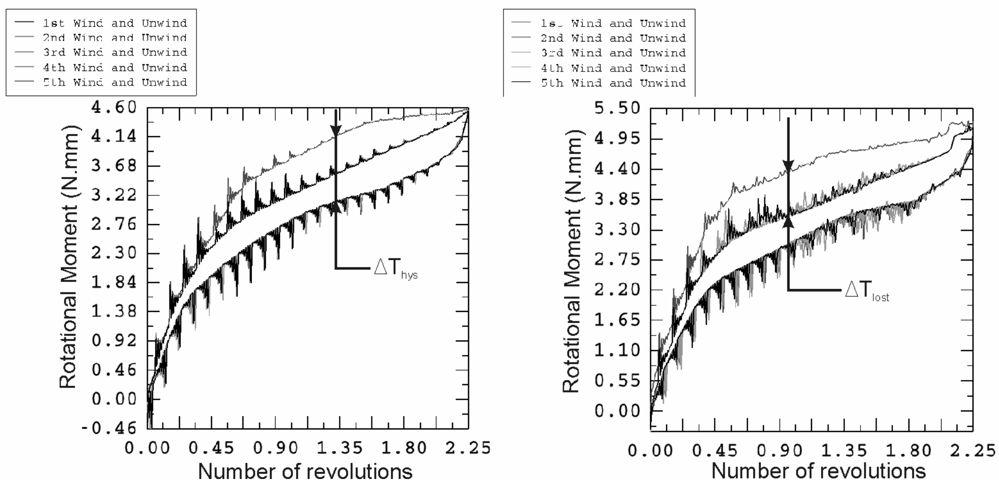

a. Perfectly plastic spring material. **b. Hardened material.**

Figure 7. Cyclic moment-rotation response plots for 2.25 revolutions of the arbor.

The magnitude of the torque lost was found to increase with material hardening. For a perfectly plastic spring material, the torque lost in successive winds was found to be significant only for the first two winds, for both the cases of wind-up (1 rev and 2.25 revs). For a hardened material, on the other hand, the latter was found to be relatively more prominent even for the subsequent winds, although it was found to decrease with the number of winds. However, for both perfect plasticity and hardening, except for the case of 2.25 revolutions -- for the first two winds and unwinds, the additional winds were observed to have negligible influence on the hysteresis loss of the spring system. Table 2 (a & b) shows a comparison of the torque lost - both in hysteresis as well as in successive winds - for a perfectly plastic spring material to that of a hardened one (for five winds and unwinds).

Friction was observed to have a negligible influence on the cyclic moment-rotation response of the spring.

Average torque lost in successive winds - ΔT_{lost} (mN.mm)				
Combination of winds	**Perfect Plasticity**		**Hardening Plasticity**	
	1 revolution	**2.25 revolutions**	**1 revolution**	**2.25 revolutions**
Wind1 - Wind2	8.28	530	28.2	550
Wind2 - Wind3	≈ 0.00	≈ 0.00	15.9	18.4
Wind3 - Wind4	≈ 0.00	≈ 0.00	14.7	15.1
Wind4 - Wind5	≈ 0.00	≈ 0.00	10.4	5.89

a. Torque lost in successive winds.

Average torque lost in hysteresis (within a cycle) - $\Delta T_{hysteresis}$ (mN.mm)				
Number of winds	**Perfect Plasticity**		**Hardening Plasticity**	
	1 revolution	**2.25 revolutions**	**1 revolution**	**2.25 revolutions**
Wind1 - Unwind1	425	1050	600	1160
Wind2 - Unwind2	425	475	600	615
Wind3 - Unwind3	425	475	600	615
Wind4 - Unwind4	425	475	600	615
Wind5 - Unwind5	425	475	600	615

b. Torque lost in hysteresis.

Table 2. Comparison of torque lost readings for different cases of material plasticity and winds.

4.4 Aging

Research was carried out to study the influence of 'aging' on a formed (wound and released) clock spring before it is used for the actual wind-up application. The objective of this modeling effort was to understand the shelf life of the spring before use. For this purpose, numerical simulations were developed which can accurately capture the 'state' of the formed spring, after sitting in the cup for several years. The results show evidence of a significant amount of stress relaxation which is proportional to the aging time. For example, an aging period of 10 years was found to relax the maximum stress in the formed spring by approximately 67%.

During the aging process, all degrees of freedom in the arbor are released (similar to the instantaneous arbor release case, mentioned earlier), and this leads to a rotational creep of the arbor in the clockwise direction, of approximately 80 mrads. The arbor is then centered-concentric with the cup (contrary to the case of a freshly formed spring), before it is used for the additional wind-ups. The torque readings so obtained were found to be much lower than those for a freshly formed (not aged) spring. Table 3 shows a comparison of the torque readings for a spring with 10 years of aging to a freshly formed spring, for the cases of perfect plasticity and 'perfect lubrication'. It can be seen that 10 years of aging reduced the torque readings significantly; by about 42% for the case of 1 revolution, and by 26% for the case of 2.25 revolutions of the arbor.

ADDITIONAL WIND-UPS →	**1 revolution**	**2.25 revolutions**
SPRING TYPE	**Torque readings (N.mm)**	
Freshly formed	3.52	4.40
Aged (for 10 Years)	2.05	3.27
Design specifications	2.9 ± 0.5	4.35 ± 0.55

Table 3. Comparison of torque readings of an aged spring to a freshly formed one.

The dissimilarity in the torque values (as given in Table 3) for the aged spring when compared to design specifications, must be considered with high priority for benchmarking the design and application of clock springs.

4.5 Long-term relaxation response

The long-term relaxation response of the clock spring is due to the effect of creep of the spring material (Elgiloy) on the structural response of the spring system as a whole. Creep properties of the spring material were captured by performing uniaxial tension tests on the elgiloy wire. The data obtained was fitted to a steady state creep power-law model, shown in Equation 1.

$$\dot{\varepsilon}_{cr} = A \cdot q^n \tag{1}$$

Where $\dot{\varepsilon}_{cr}$ is the creep strain rate (S^{-1}),

q is the von-Mises equivalent stress (MPa),

A , n are the power-law creep parameters (assumed to be material constants).

Curve fitting of rates determined at different levels of uniaxial stress, leads to values of A and n as 6E-18 $MPa^{-2.24}S^{-1}$, and 2.24, respectively.

The long-term response of the actual spring system, incorporating this steady state creep behavior is obtained, about a pre-loaded (wound-up) state. Based on the results, the springs were observed to undergo significant stress relaxation over an extended period of time (of the order of several years), which in-turn leads to a drop in the value of torque at a given value of rotation. This drop in the torque is quantified by the decrease in the reactional rotational moment of the arbor. As expected, the spring system at 2.25 revolutions of the arbor resulted in a higher torque-drop compared to 1 revolution, due to the higher initial stress state of the former case. Material hardening was found to increase this drop significantly, whereas, lubrication was found to reduce this effect to a lower extent. Aging (before wind-up) was found to reduce the torque drop significantly (as discussed in page-12). Based on these findings, residual stresses and frictional self contact were observed to be the key contributors that influence this long-term structural response.

The results obtained for a freshly formed spring, indicated an average rate of torque drop of approximately 1.6 - 2.5 mN.mm per day for the case of 1 revolution, and approximately 2.5 - 3.3 mN.mm per day for the case of 2.25 revolutions of the arbor. Table 4 shows a comparison of the values of torque drop for a freshly formed spring over varying time periods of relaxation, levels of wind-up, and different cases of material plasticity and lubrication.

Wind-up positions	**Time (days)**	**Perfect Plasticity**		**Hardening Plasticity**	
		Perfect lubrication	**No lubrication**	**Perfect lubrication**	**No lubrication**
ΔT_{creep} 1 revolution (mN.mm)	**1**	2.01	2.28	2.97	3.27
	12	24.0	27.4	35.4	39.2
	365 (1 year)	590	666	827	908
ΔT_{creep} 2.25 revolutions (mN.mm)	**1**	3.31	3.50	4.04	4.77
	12	39.4	41.7	47.9	64.4
	365 (1 year)	913	966	1080	1213

Table 4. Comparison of the torque drop values for a freshly formed spring, for different cases of material plasticity, lubrication, and windups.

The torque drop results obtained from the FE model were compared to the experimental results. Figure 8 shows a comparison of the FE results for a freshly formed spring (for a wind-up of 1 revolution) - made of a perfectly plastic spring material (and with ‘perfect lubrication’) - to the experimental results; for a stress relaxation period of 12 days. The FE results estimated about 15 times higher torque drop (for 12 days) compared to experiments, for the case of 1 revolution. It should be noted that the experimental results also include primary creep which is not considered in the FE model.

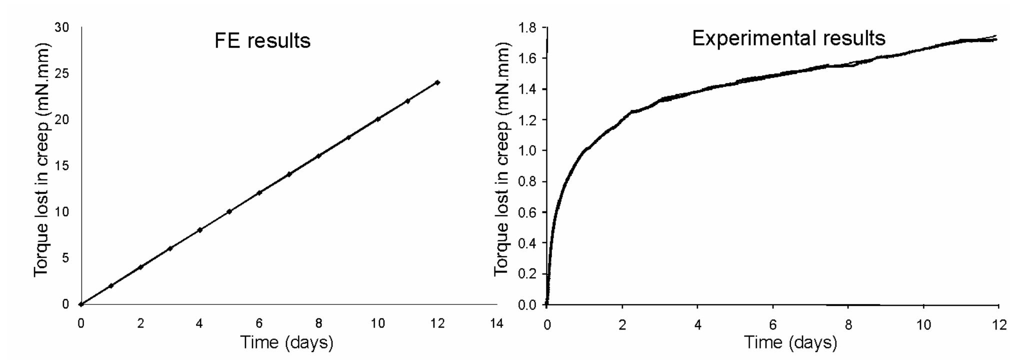

Figure 8. Comparison of FE results (for a freshly formed spring) with the experimental results showing torque drop response over a period of 12 days.

For a period of 1 year of stress relaxation -- for a freshly formed spring-- the FE model predicted 25 and 46 times higher torque drop compared to experiments, respectively for the cases of 1 revolution and 2.25 revolutions of additional wind-ups. On the other hand, for a spring aged for 10 years, these values dropped to 10 and 26 times (compared to experiments), respectively for the same wind-up levels. Table 5 shows the torque drop results for 1 year of stress relaxation, for a perfectly plastic spring material and using ‘perfect lubrication’.

ADDITIONAL WIND-UPS →	1 revolution	2.25 revolutions
SPRING TYPE	Torque-drop readings (mN.mm)	
Freshly formed	590	913
Aged (10 Years)	193	528
Experimental results	≈ 20	≈ 20

Table 5. Comparison of the torque drop values (over 1 year) for a freshly formed spring to a 10 years aged spring, for perfect plasticity and perfect lubrication

The discrepancy in the torque drop values (as shown in Table 5) is under investigation, but we outline two likely reasons:

1. Inaccuracy in the determination of material creep parameters, from experiments.

    - The elgiloy creep parameters, determined from the uniaxial tension tests, drive the FE model for capturing the long-term spring response. However, recent tests carried out suggest that actual steady-state rates of creep may be smaller than previously measured. This can have a remarkable influence on the torque drop.

2. Variation of the span of shelf life (aging).

    - There is variation in the actual shelf life of the springs before they are used. As discussed earlier, the time period of aging has a strong influence on the torque drop readings. Torque drop results for aging gave evidence of an exponential decay with the increasing aging time.

The FE results for 1 year of stress relaxation predicted an average stress relaxation of about 20% for a freshly formed spring, and about 12% for a spring aged for 10 years, for an additional wind-up of 1 revolution.

5. Analytical Model

The objective of this modeling effort is to use simple techniques from the principles of statics and mechanics of solids to develop an analytical model that will approximately describe the long-term relaxation response of the torsional spring about a preloaded state. The ultimate goal of this effort is to develop a ***Moment-Rotation Creep Law*** which can predict the instantaneous as well as long-term moment-rotation response of a typical torsional spring system, accounting for parameters related to geometry, frictional coefficient and material creep.

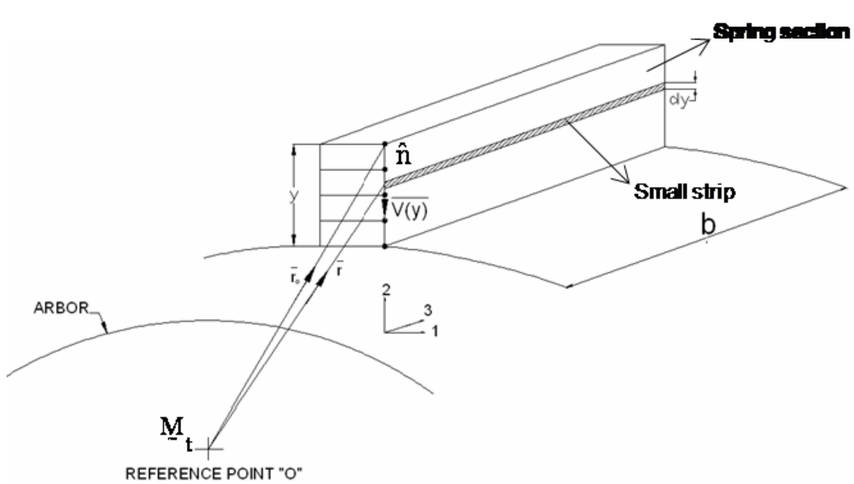

Figure 9. A schematic of a section of the torsional spring (for analytical model)

For this purpose, a typical cross-section of a freshly-formed torsional spring (wound-up at 1 revolution) is considered, and an analytical model is developed based on the static equilibrium of the arbor and the portion of the spring from the arbor to the cross-section considered (shown in Figure 9). Triad 1-2-3 refers to the local coordinate system associated with the spring cross-section, with axis-1 being normal to the plane of the section.

We employ the equations of planar static equilibrium which result in the following relations among the components of the reaction forces and moments at the arbor center, and the sectional forces and moments at the cross-section considered.

$$\text{i.e. } \Sigma \underset{\sim}{F} = 0 \text{ and } \Sigma \underset{\sim}{M} = 0 \tag{2}$$

$$RF1 = SOF1,\ RF2 = SOF2,\ RM3 = SOM3 \tag{3}$$

Where $RF1$ and $RF2$ are the components of the reaction force at the arbor center,

$RM3$ is the reaction moment at the arbor center,

$SOF1$, $SOF2$ and $SOM3$ are the sectional forces and moment at the spring cross-section considered.

The instantaneous static moment response of the spring system can be computed by considering a small strip of the spring material within the section. This strip has thickness- dy and width- b (as shown in Figure 9). The effective sectional force on the entire spring section is the integral of the net force acting on this small strip, evaluated through the thickness of the section. The normal and tangential components of the net force acting on the strip, in the local coordinate system 1-2-3, are derived from their corresponding instantaneous stress components, as shown in Equation 6. The instantaneous moment contribution of the section at the arbor center is then calculated as an integral of the cross product of the moment arm of the strip (with respect to the arbor center) with the net effective force acting on the strip, as shown in Equation 7. Equations 4 & 5 show the derivations for the moment arm.

$$\underset{\sim}{r} = \underset{\sim}{r}_0 + \underset{\sim}{y}(y) \tag{4}$$

$$\underset{\sim}{y}(y) = y\hat{n} \tag{5}$$

$$d\underset{\sim}{F} = \sigma_n(y,0)\cdot b\cdot dy\cdot \underset{\sim}{e}_1 + \sigma_s(y,0)\cdot b\cdot dy\cdot \underset{\sim}{e}_2 \tag{6}$$

$$M_0 = \int_y (\underset{\sim}{r}\times d\underset{\sim}{F})\cdot \underset{\sim}{e}_3 \tag{7}$$

Where $\underset{\sim}{r}$ is the moment arm vector of the small strip about the arbor center,

$\underset{\sim}{r}_0$ is a fixed vector of the upper end of the section about the arbor center,

y is a variable representing position along the thickness of the section,

$\underset{\sim}{y}(y)$ is a vector representing variation of position along the thickness of the section, in the direction of unit tangential vector $\hat{n}$,

$\underset{\sim}{dF}$ is the net force acting on the small strip of the section,

$\sigma_n(y,0)$ is the instantaneous stress component normal to the cross-section,
$\sigma_s(y,0)$ is the instantaneous stress component tangential to the cross-section,

$\underset{\sim}{M}_0$ is the net instantaneous moment of the sectional forces about the arbor center.

Numerical integration techniques like the Gauss-Lobatto method and Simpson's rule were used for evaluating the integral shown in Equation 7. For this purpose, the normal and shear stresses extrapolated at the nodes of the section (in the local 1-2-3) by the finite element discretization method were used, in conjunction with their corresponding moment arms about the arbor center. The result for the instantaneous moment was found to be in good agreement with the corresponding finite element result. The Simpson's rule gave an error of only 1.2%, whereas the Gauss-Lobatto method gave about 3.5%, in comparison to the FE results (for a freshly formed spring).

Once the instantaneous moment was captured, the next stage in the analytical work was to determine the long-term moment of the torsional spring caused due to stress relaxation. Following the approach used above, the goal was to determine the expressions for stresses at the cross-section, after allowing the system to relax over a period of time. The latter, which are functions of the position along the section thickness and time, were derived from the power law expression for the creep strain rate, shown earlier in Equation 1. Since the creep parameter $n \neq 1$, the expressions for stresses follow Equations 8 and 9.

$$\sigma_n(y,t) = \sigma_n(y,0) \cdot \left[1 + \frac{(n-1).A.E.t}{\sigma_n(y,0)^{(1-n)}} \right]^{\frac{1}{1-n}} \tag{8}$$

$$\sigma_s(y,t) = \sigma_s(y,0) \cdot \left[1 + \frac{(n-1).A.E.t}{\sigma_s(y,0)^{(1-n)}} \right]^{\frac{1}{1-n}} \tag{9}$$

Where $\sigma_n(y,t)$ is the long-term stress component normal to the cross-section,

$\sigma_s(y,t)$ is the long-term stress component tangential to the cross-section,

E is the Young's modulus of the Elgiloy material.

Using the non-linear expressions for stresses derived in Equations 8 and 9, and following the strategy used for the instantaneous case, the expression for the long-term moment of the spring system was derived, as shown in Equation 10. Equation 11 shows the expression for the corresponding torque drop due to long-term stress relaxation.

$$\underset{\sim}{M}_t = \int_y (\underset{\sim}{r}_0 + \underset{\sim}{y}(y)) \times \left(\sigma_n(y,0)\cdot\left[1+\frac{(n-1).A.E.t}{\sigma_n(y,0)^{(1-n)}}\right]^{\frac{1}{1-n}}\cdot\underset{\sim}{e}_1 + \sigma_s(y,0)\cdot\left[1+\frac{(n-1).A.E.t}{\sigma_s(y,0)^{(1-n)}}\right]^{\frac{1}{1-n}}\cdot\underset{\sim}{e}_2\right)\cdot b\cdot dy \tag{10}$$

$$\Delta T_{cr} = (\underset{\sim}{M}_0 - \underset{\sim}{M}_t)\cdot\underset{\sim}{e}_3 \tag{11}$$

Where ΔT_{cr} is the torque drop due to stress relaxation.

Simpson's rule was used to evaluate the above integral. The results obtained were found to be in good agreement with the finite element results. Figure 10 shows a comparison of the torque drop values for a freshly formed spring - for the additional wind-up of 1 revolution - over a period of 1 year of stress relaxation, obtained from the analytical model with the corresponding FE results. The long-term moment was found to be nearly linear for smaller periods of time of the order of weeks to months and non-linear for larger time periods.

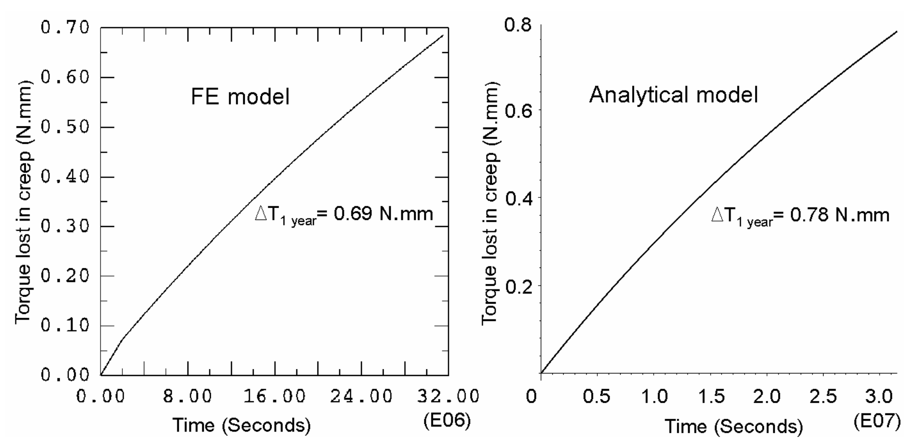

Figure 10. Comparison of FE results with the analytical results for torque drop response over a period of 1 year for a freshly formed spring.

The analytical model estimated a torque drop of approximately 33.5 mN.mm over a period of 12 days, and approximately 780 mN.mm over a period of 1 year, which are in good agreement with the FE results shown earlier in Table 3 (for a freshly formed spring, and additional wind-up of 1 revolution). The associated stress relaxation was estimated at about 10% at the end of 12 days, and about 24% at the end of one year.

Hence, it was observed that the analytical model estimated the same magnitude of torque drop and stress relaxation as the FE model for the torsional spring.

6. Conclusions

This paper describes the development of a detailed component-level finite element model for a torsional spring system, to investigate the instantaneous static moment-rotation response and the long-term relaxation response. Non-linear material behavior (plasticity and creep) was found to be the major contributor influencing this response. Friction and large deformations appear to make relatively smaller contributions. The static response captured by the FE model was found to be in good agreement with the experimental results and the design specifications, whereas, the creep response was found to agree with the results of the analytical model. FE results for a freshly-formed spring predict an average torque-drop rate of approximately 1.6 - 3.3 mN.mm/day, depending on the magnitude of loading, and conditions of friction and material plasticity. Aging was found to reduce these readings significantly. These springs were also observed to exhibit significant hysteresis when subjected to rotation-controlled loading and unloading cycles.

7. References

1. Abaqus/Standard Analysis User's Manual, "Two dimensional solid element library," chapter. 22.1.3, Version 6.6, Version 6.7, 2007.
2. Assefpour-Dezfuly, M., Bonfield, W., "Strengthening mechanisms in elgiloy," Journal of Material Science, vol. 19, pp. 2815-36, 1984.
3. Assefpour-Dezfuly, M., Bonfield, W., "Microplasticity in elgiloy," Journal of Material Science, vol. 20, pp. 3018-26, 1985.
4. Dalder, E., "Tensile properties of elgiloy strip," U.C. Berkeley: Faxed data from Lawrence Livermore National Laboratory, 2003.
5. Dykhuizen, R.C., Robino, C.V., "Load relaxation of helical extension springs," Journal of Material Engineering Performance, vol. 13, pp. 151-7, 2004.
6. Lawton, K.M., Lynn K.C., Ren, D., "The measurement of creep of elgiloy springs with a balanced interferometer," Journal of Precision Engineering, vol. 31, pp. 325-329, 2007.

8. Acknowledgement

The authors gratefully acknowledge financial support from The Lawrence Livermore National Laboratory. They also acknowledge Dassault Systemes SIMULIA corp. for permitting the use of Abaqus through an academic license.